JACS
JOURNAL OF THE AMERICAN CHEMICAL SOCIETY

Article

pubs.acs.org/JACS

Hückel Theory and Optical Activity

Veronica L. Murphy and Bart Kahr*

Department of Chemistry and Molecular Design Institute, New York University, 100 Washington Square East, Silver Center, Room 1001, New York, New York 10003, United States

Supporting Information

ABSTRACT: Optical rotations and rotatory strengths are calculated for achiral, conjugated hydrocarbons with the aim of determining to what extent the sum-over-$\pi \rightarrow \pi^*$ rotatory strengths are sufficient to account for nonresonant optical activity. The separability of σ and π electrons might provide a short cut to the interpretation of chiroptical structure−property relations in some cases. It is shown that by restricting the analyses to planar, C_{2v}-symmetric π-systems and their one electron HOMO−LUMO excitations, an intuitive understanding of the vexing property of optical activity is forthcoming for the following reasons: Hückel wave functions are simply calculated, and in some cases, they can even be approximated by inspection of structure. Wave functions of planar molecules can be multiplied with one another graphically or, in the mind's eye, to yield transition electric and magnetic moments. The gyration tensors have just one independent component. Transition dipole moments are orthogonal to one another. And, the most optically active directions are found at their bisectors. Throughout, emphasis is on the evaluation of long wavelength optical rotation, consistent with quantum chemical computation, using simple models that are part of the fabric of organic chemistry pedagogy.

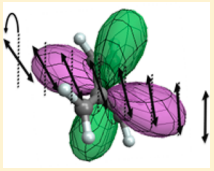

INTRODUCTION

Hückel theory is an approximate molecular orbital theory for planar, conjugated hydrocarbons, whereas optical activity is typically associated with molecular chirality, a consequence of bonding in three dimensions. Hückel theory and optical activity are subjects that at first blush brook no intersection. Why the conjunction "and" in the title?

Giving voice to signs and magnitudes of specific rotations of organic compounds has challenged scientists for 200 years, ever since Biot discovered in 1815 that solutions of some organic compounds are optically active.[1] Subsequently, we have not been able to interpret observed values of solution optical activity in simple terms. The room temperature, sodium *D*-line, specific rotation of (2*R*,3*R*)-tartaric acid is +12°, but there is not a scientist in the world who can say why it is +12 rather than −12 or even −120, on the basis of the simple inspection of structure. Thus, we have been perennially teaching students how to assign molar and specific rotations—in effect random numbers—to compounds without explanation of how and why they arise in a particular structure. This is a pedagogical scandal.

Our long-standing ignorance has its origins in both experimental and theoretical impediments. We take aim only at the latter here, but a few remarks about experiment are requisite. Solution rotations are averages of *bisignate* tensorial quantities. The average value of a set of positive and negative numbers can be many things. By contrast, average values of chemical shielding tensors are readily interpretable. This is because shielding tensors are *monosignate*; if one component is large, the average is large. For bisignate quantities, average values cannot be reckoned unless we know what we are averaging. This requires measurements on *oriented* structures. We have been working to improve experimental methods for delivering this information[2,3] following in the wake of others.[4−7]

Typically, contemporary calculations of optical activity tensors are reduced to pseudoscalars for ease of comparisons with solution data.[8−10] Incisive schemes have been directed at the interpretation of spatial averages of chiral molecules,[11−14] but achiral molecules challenge the wisdom of this reduction. The spatial average of the optical activity of *all* achiral, optically active molecules is zero. This means that we can make *no* distinctions within this class of optically active compounds from solution measurements alone.

Herein, we make no concessions to chirality or average values by focusing on oriented, planar π-systems. We do so for the following reasons: (1) Wave functions under the Hückel approximations are simply written down or calculated by pencil and paper. (2) It is easy to graphically compute products of filled and unfilled π orbitals for planar structures, a necessary procedure for deriving transition moments. (3) The absolute (sign indifferent) shapes of optical activity tensor representation surfaces are given by symmetry and are defined by a single independent component in the point group C_{2v}. (4) Transition electric dipole and magnetic dipole moments are orthogonal to one another, with the most optically active directions found at the bisectors. With all this in favor of achiral molecules, it is a wonder that chemists first tried to understand optical activity of chiral compounds with twisted wave functions and transition moments disposed in seemingly arbitrary directions. This is a historical misfortune that arose merely from the overwhelming preponderance of chiroptical measurements of solutions.

Optical activity of oriented, nonenantiomorphous structures of symmetry S_4 and D_{2d} was predicted in 1882 by Gibbs.[15] In the process of systematizing crystal physics, Voigt extended Gibbs' prediction to groups C_{2v} and C_s.[16] The conjecture of Gibbs and

Received: February 16, 2015
Published: March 23, 2015

DOI: 10.1021/jacs.5b01763
J. Am. Chem. Soc. 2015, 137, 5177−5183

Voigt that oriented, achiral systems could be optically active was verified by experiment for crystals in 1962.[17,18] The first quantitative theoretical evaluation of optical activity of a specific achiral *molecule* was of *cis*-butadiene.[19] The computation of the rotatory strength tensor for a $\pi \rightarrow \pi^*$ transition revealed that, although the trace of the tensor was zero, there was a unique off-diagonal component with a relatively large value. This work was followed by a computational study of formaldehyde, likewise with one nonvanishing tensor element.[20] Few measurements of the optical activity of achiral molecules have been reported.[21,22] The experimental determination of the full optical activity anisotropy associated with an achiral molecule is from that of pentaerythritol in achiral crystals.[14,23] (Optical activities of other achiral crystals have been determined, but these are not built from discrete molecules.[24]) Surprisingly, optical rotation (OR) was observed from polar layers of the planar nematic *para*-azoxyanisole inclined by ±7° from a plane of symmetry, even though the mesogens themselves are nearly centrosymmetric.[25,26] A more compelling example comes from the bent core banana liquid crystal phases.[27] Nonlinear optical activity was observed in polar monolayers of an achiral nitropyridine derivative.[28] Nanofabricated and meta- materials are proving to be rich in chiroptical phenomena, even in the absence of chirality, but this subject is only loosely connected to molecular chiroptics.[29]

We here aim to use achiral molecules to more clearly articulate chiroptical structure/property relationships. The difficulty of explaining long wavelength optical activity in terms of electronic structure lies in the fact that many excitations far from resonance contribute to the response at low energy. Indeed, rotatory strengths of hundreds of excitations had to be summed to achieve convergence with the results of the linear response method for a variety of small, chiral, organic compounds such as substituted oxiranes[30] and amino acids.[31] Likewise, we had observed that the computed OR for pentaerythritol did not match that obtained from our measurements on single crystals[23] until first summing the contributions of >200 excitations.[14]

On the other hand, the rotatory strength of the first excitation of (1*S*,4*S*)-norbornenone seemed to be a reasonable approximation to the overall OR.[30,32−34] It is thus unclear when a vast summation is required for predicting the long wavelength OR for all compounds and all classes of compounds.

Computers can carry knowledge of many molecular wave functions, but human beings cannot. Thus, predictions of OR delivered by recent advances in chiroptical theory[35] often lie behind advanced computing engines and highly refined electronic structure calculation algorithms. Answers are not always easily explained.

Here, we continue to seek shortcuts for particular molecules that affect interpretation (structure−property relationships) that actualize thinking about the interactions of light and matter in the absence of massive computation. Such models, although only semiquantitative, are an essential part of understanding and should become part of the pedagogical foundation of organic chemistry. In 2007, we determined that a structure-based understanding of OR could be reached for molecules for which we have an intuitive understanding of electronic structure, that is, molecules for which we can write down approximations of the wave functions straightaway. The average chemist can do this for diatomics and triatomics but for little else. For this reason, we examined the OR of the simplest optically active compound of common experience, H_2O, on the basis of judgments that could be drawn from chalkboard wave functions.[21] With the orbitals in hand, the moments were easily derived by the graphical procedure of Snatzke (see Figure 1), leading to the qualitative predictions of the anisotropy of OR for any one-electron excitation, without resorting to numerical computation.[36] At the same time, this exercise left us wanting because triatomics do not carry us far into organic chemistry.

There is an important class of organic compounds for which chemists do have an intuitive understanding of electronic structure in part: planar conjugated hydrocarbons. Many such compounds belong to optically active, nonenantiomorphous point groups (Scheme 1).[22] π wave functions can be estimated by inspection of structure or derived by back-of-the-envelope Hückel calculations. If the sum-over-$\pi \rightarrow \pi^*$ excitations is sufficient for approximating long-wavelength ORs, then we will have broached a large class of molecules, central to organic chemistry pedagogy, whose ORs should be readily interpretable.

Scheme 1. Achrial, Conjugated Hydrocarbons[a]

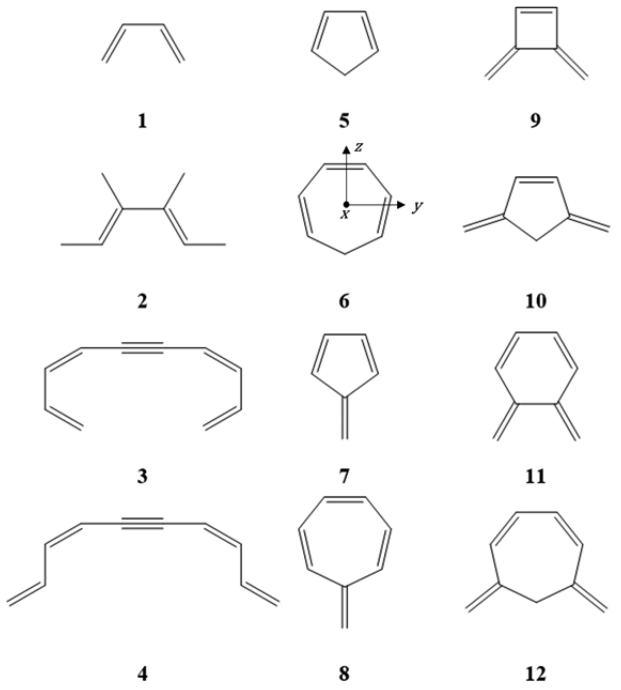

[a] **1**, *cis*-butadiene; **2**, (2*E*,4*E*)-3,4-dimethyl-2,4-hexadiene; **3**, (3*Z*,7*Z*)-deca-1,3,7,9-tetraen-5-yne; **4**, (3*Z*,7*Z*)-deca-1,3,7,9-tetraen-5-yne; **5**, cyclopentadiene; **6**, cyclohexatriene; **7**, fulvene; **8**, 7-methylene-1,3,5-cycloheptatriene; **9**, 3,4-dimethylene-1-cyclobutadiene; **10**, 3,5-dimethylene-1-cyclopentene; **11**, 5,6-dimethylene-1,3-cyclohexadiene; **12**, 5,7-dimethylene-1,3-cycloheptadiene. The *x* axis is perpendicular to the molecular plane, and *z* is the C_2 axis for all compounds. See structure **6**.

THEORETICAL BACKGROUND

Optical rotation and circular dichroism (CD) are consequences of the interactions of transition electric dipole moments ($\boldsymbol{\mu}$) with transition magnetic dipole moments ($\mathbf{m}$), and transition electric quadrupole moments ($\boldsymbol{\Theta}$). OR anisotropy is proportional to the gyration tensor, $\mathbf{g}_{\alpha\beta}$.[37]

$$\mathbf{g}_{\alpha\beta} = \frac{1}{4E}\left\{\varepsilon_{\alpha\gamma\delta}\left[\frac{1}{3}E(A_{\gamma\delta\beta} - A_{\delta\gamma\beta}) + \varepsilon_{\lambda\beta\gamma}G'_{\delta\lambda} - \varepsilon_{\lambda\beta\delta}G'_{\gamma\lambda}\right]\right\} \quad (1)$$

DOI: 10.1021/jacs.5b01763
J. Am. Chem. Soc. 2015, 137, 5177−5183

Here, ε is the Levi−Civita operator, E is the energy of the nonresonant excitation, G' is the $\boldsymbol{\mu}-\mathbf{m}$ polarizability and A is the $\boldsymbol{\mu}-\boldsymbol{\Theta}$ polarizability. Einstein summations over all combinations are implied. The tensors $\mathbf{G}'$ and $\mathbf{A}$ are defined as

$$\mathbf{G}'_{\alpha\beta} = -2E \sum_{j\neq n} \mathrm{Im}\frac{\langle n|\mu_\alpha|j\rangle\langle j|m_\beta|n\rangle}{{E_{jn}}^2 - E^2} \tag{2}$$

$$\mathbf{A}_{\alpha\beta\gamma} = 2 \sum_{j\neq n} E_{jn} Re\frac{\langle n|\mu_\alpha|j\rangle\langle j|\Theta_{\beta\gamma}|n\rangle}{{E_{jn}}^2 - E^2} \tag{3}$$

where j and n represent molecular wave functions and E_{jn} is the excitation energy of a transiton from j to n.

CD anisotropy is proportional to the rotatory strength tensor,

$$\mathbf{R}^{jn}_{\alpha\beta} = -\frac{1}{2}\left\{\varepsilon_{\alpha\gamma\delta}\left[\frac{1}{3}E_{jn}(V_{\gamma\delta\beta} - V_{\delta\gamma\beta}) - \varepsilon_{\lambda\beta\gamma}U_{\delta\lambda} + \varepsilon_{\lambda\beta\delta}U_{\gamma\lambda}\right]\right\} \tag{4}$$

where U and V are defined as

$$U_{\alpha\beta} = \mathrm{Im}\langle n|\mu_\alpha|j\rangle\langle j|m_\beta|n\rangle \tag{5}$$

$$V_{\alpha\beta\gamma} = \mathrm{Re}\langle n|\mu_\alpha|j\rangle\langle j|\Theta_{\beta\gamma}|n\rangle \tag{6}$$

By combining eqs 1−6, the gyration tensor is shown to be a result of summing the rotatory strength tensors over all excited states (see S4 in the Supporting Information (SI) for stepwise derivation from eq 1).

$$\mathbf{g}_{\alpha\beta} = -\sum_{j\neq n} \frac{R^{jn}_{\alpha\beta}}{{E_{jn}}^2 - E^2} \tag{7}$$

Equations assume that the components are reported in atomic units. Conversion to cgs or SI units requires the addition of fundamental constants. All calculations herein were performed using Gaussian09, version B.01 (see S1 in the Supporting Information for complete citation). Rotatory strengths are reported in cgs units where gyration tensors are in atomic units. To avoid extensive unit conversion, gyration tensors are constructed from the induced multipolar moments reported in the rotatory strength output in atomic units according to

$$\mathbf{g}_{\alpha\beta} = \frac{1}{2}\sum \frac{1}{E_{jn}^2 - E^2}\left\{\varepsilon_{\alpha\gamma\delta}\left[\frac{1}{3}E_{jn}(\mu_\gamma\Theta_{\delta\beta} - \mu_\delta\Theta_{\gamma\beta}) - \varepsilon_{\lambda\beta\gamma}\mu_\delta m_\lambda + \varepsilon_{\lambda\beta\delta}\mu_\gamma m_\lambda\right]\right\} \tag{8}$$

Gaussian09 does not output the induced moments $\boldsymbol{\mu}$, $\mathbf{m}$, and $\boldsymbol{\Theta}$ directly, but rather, the matrix elements associated with the operators ∇, $\mathbf{r}\times\nabla$, and $\nabla\mathbf{r} + \mathbf{r}\nabla$, respectively. By combining the operator expressions with the appropriate constants,[37,38] the moments follow as

$$\boldsymbol{\mu} = \frac{\nabla}{E_{jn}} \tag{9}$$

$$\mathbf{m} = \frac{r\times\nabla}{2} \tag{10}$$

$$\boldsymbol{\Theta} = \frac{3(\nabla r + r\nabla)}{2E_{jn}} \tag{11}$$

E_{jn} is in hartrees.

The $g_{\alpha\beta}$ component equation is usually specified in terms of the g_{zz} component only.[32,37,39]

$$g_{zz} = \sum \frac{1}{{E_{jn}}^2 - E^2}\left[\frac{1}{3}E_{jn}(\mu_x\Theta_{yz} - \mu_y\Theta_{xz}) - \mu_x m_x - \mu_y m_y\right] \tag{12}$$

(See S4 in the SI for stepwise derivation from eq 8.) However, molecules with symmetry C_{2v} will always have $g_{zz} = 0$. The only independent nonzero tensor component for C_{2v} molecules is $g_{xy} = g_{yx}$. Therefore, we concern ourselves with only the symmetrized g_{xy} component equation.

$$g_{xy} = \frac{1}{2}\sum \frac{1}{E_{jn}^2 - E^2}\left[\frac{1}{3}E_{jn}(\mu_y\Theta_{zy} - \mu_z\Theta_{xx} - \mu_z\Theta_{yy} - \mu_x\Theta_{zx}) + \mu_x m_y + \mu_y m_x\right] \tag{13}$$

(See S4 in the SI for stepwise derivation from 8.) To compare $\boldsymbol{\mu}-\mathbf{m}$ and $\boldsymbol{\mu}-\boldsymbol{\Theta}$ interactions, we must separate g_{xy} into its parts:

$$g_{xy} = g^m_{xy} + g^\Theta_{xy} \tag{14}$$

where

$$g^m_{xy} = -\frac{1}{2}\sum \frac{1}{{E_{jn}}^2 - E^2}(\mu_x m_y + \mu_y m_x) \tag{15}$$

$$g^\Theta_{xy} = \frac{1}{6}\sum \frac{E_{jn}}{{E_{jn}}^2 - E^2}(\mu_y\Theta_{zy} + \mu_z\Theta_{xx} - \mu_z\Theta_{yy} - \mu_x\Theta_{zx}) \tag{16}$$

Once the individual interactions are separated, we can use the predicted tensor components in eqs 15 and 16 and the geometry of the chemical structures to describe OR based on the induced multipolar moments. To describe relative transition moments generated during the $\pi \rightarrow \pi^*$ transitions of each structure, we have used Snatzke's[36] method (illustrated for **10** in Figure 1a) for the interpretation of charge movement. For a one-electron excitation between two molecular orbitals, negative charge builds where orbitals overlap in phase and is depleted where orbitals overlap out of phase. Hückel coefficients of the π and π^* orbitals can be used to quantify this movement (Figures 1b and 1c). The relative magnitudes of $\boldsymbol{\mu}$ and $\mathbf{m}$ for conjugated ∩-shaped molecules in our set **1**−**12** (Scheme 1) can be estimated from the separation of the atoms with the largest charge enhancement and depletion.

Finally, for reckoning the gyration tensor with experimental solution data (where available), we must convert the gyration to OR (ϕ),[35a]

$$\phi = \frac{4\pi N\beta(n^2 + 2)}{3Ec^2} \tag{17}$$

where ϕ is the OR, N is the number of molecules per unit volume, n is the refractive index, c is the speed of light (which is 1 if the gyration tensor remains in atomic units), and β is the average of the $\mathbf{G}'$ tensor eigenvalues divided by the energy (E).

$$\beta = -\frac{G'_{xx} + G'_{yy} + G'_{zz}}{3E} \tag{18}$$

To translate this to OR in a particular direction, β becomes the tensor component of g in the desired direction divided by $-E$. Therefore, direction-dependent OR is

DOI: 10.1021/jacs.5b01763
J. Am. Chem. Soc. 2015, 137, 5177−5183

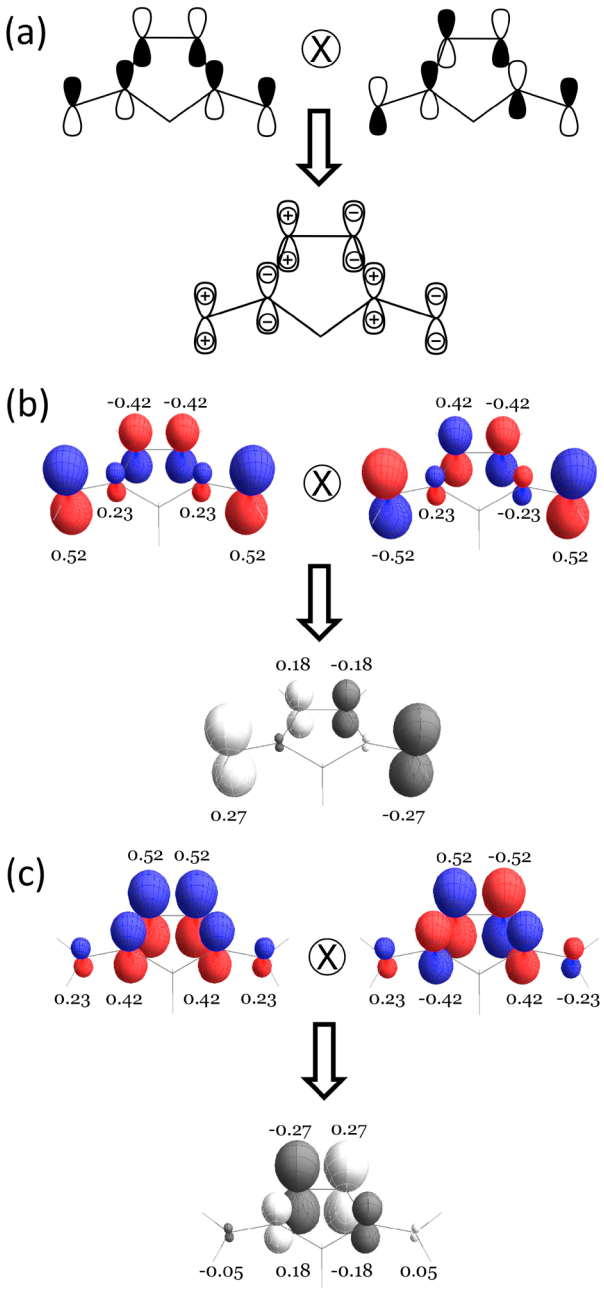

Figure 1. (a) Scheme of overlap density predicted from HOMO−LUMO product of **10**. (b) Overlap density as in part a but based on Hückel coefficients. (c) $\pi_1 \rightarrow \pi_6^*$ overlap density. Charge separation in part b is greater than in part c by this analysis, leading to a larger $\boldsymbol{\mu}$. The magnetic moment **m** will be larger, in turn.

$$\phi_{\alpha\beta} = -\frac{4\pi N g_{\alpha\beta}(n^2+2)}{3E^2c^2} \tag{19}$$

This equation shows that there is a negative relationship between gyration and OR, meaning that $-g_{\alpha\beta}$ corresponds to dextrorotation in the $\alpha\beta$ direction, and $+g_{\alpha\beta}$ corresponds to levorotation.

RESULTS AND DISCUSSION

Sum-Over-States vs Linear Response Theory. Achiral, conjugated hydrocarbons were optimized with symmetry constraints at the B3LYP level of theory using the 6-311+G** basis set. These structures were used to calculate long-wavelength (633 nm) $g_{\alpha\beta}$ as well as $R^{jn}_{\alpha\beta}$ for 1000−2000 excited states (see S3 in the SI for details) using both the 6-311+G** and aug-cc-pVDZ basis sets. Light of 633 nm is to the low energy side of the lowest energy transition in all compounds **1**−**12**.

The DFT orbitals were compared with those derived from simple Hückel theory. DFT excited states dominated by one-electron $\pi \rightarrow \pi^*$ transitions (according to configuration interaction coefficients) were thereafter designated as $\pi \rightarrow \pi^*$ for our purposes herein. In all cases, the excited state determined to be the Hückel predicted HOMO → LUMO transition consisted of *only* that one electron transition.

The gyration tensor of each molecule was constructed from the induced multipolar moments in three ways: as sums over all available states (SOS), as sums over all $\pi \rightarrow \pi^*$ designated excited states, and from the Hückel-predicted HOMO → LUMO excited state. These tensors were then compared with the gyration tensor predicted by linear response theory (LRT) (Table 1). Only the nonzero g_{xy} tensor components are reported.

Table 1. Computed Gyration Tensors (g_{xy}, bohr^4)

	633 nm, aug-cc-pVDZ			
	LRT	SOS	π	H → L[a]
1	−14.0	−13.6	−19.3	−19.8
2	−16.4	−15.7	−21.0	−21.0
3	−136.1	−133.0	−141.9	−155.6
4	−166.4	−161.9	−171.0	−196.8
5	−6.0	−5.8	−4.8	−8.5
6	−60.9	−59.6	−65.0	−66.4
7	−10.1	−9.8	−8.5	−8.2
8	−65.4	−63.6	−67.0	−57.5
9	−9.6	−9.2	−11.1	−7.2
10	−24.0	−23.7	−31.5	−36.4
11	−80.3	−78.4	−82.1	−85.5
12	−193.5	−189.0	−189.2	−214.0

[a]HOMO → LUMO transition corresponding to the lowest energy excitation predicted by DFT, except for **9**, for which the second-lowest energy transition is the dominant state.

g_{xy} computed with LRT and as a SOS agreed to within |4%|, as anticipated; they both aim to deliver OR accurately. This comparison illustrates the validity of the equations used for all SOS calculations. SOS plots typically converged (varied ≪1 bohr^4) at fewer than 1000 states (see S113−S136 in the SI).

OR derived only from sum-over designated-$\pi \rightarrow \pi^*$ states differed, on average, by |13%|. In each case, the sign of the effect was matched direction for direction. Considering that only 4−25 Hückel-like excitations were summed rather than the 1000+ for SOS, we conclude that for simple, achiral, conjugated hydrocarbons, only the higher-lying occupied orbitals containing the most polarizable π-electrons are sufficient for the semi-quantitative accounting of long wavelength OR. The separability of σ and π electrons has a long, simplifying tradition in organic chemistry, and it serves in that capacity here.

Among the small number of $\pi \rightarrow \pi^*$-like excitations, the Hückel HOMO → LUMO transition was vastly more important in each case. OR derived from this one transition differed, on average, by only |22%|. We stress that our goal here is not numerical accuracy employing the highest levels of theory but, rather, to find paths through the thickets of electronic structure to interpret fundamental chiroptical light−matter interactions, especially for students new to the subject. Given that this single

DOI: 10.1021/jacs.5b01763
J. Am. Chem. Soc. 2015, 137, 5177−5183

Table 2. Computed Components of Gyration Tensors, g^{m}_{xy} and g^{Θ}_{xy} (bohr^4)

	633 nm, aug-cc-pVDZ							
	g^{m}_{xy}				g^{Θ}_{xy}			
	LRT	SOS	π	H → L	LRT	SOS	π	H → L
1	−11.8	−11.5	−13.6	−13.1	−2.2	−2.1	−5.7	−6.7
2	−9.0	−9.1	−7.5	−7.5	−7.4	−6.6	−13.5	−13.4
3	−129.2	−126.7	−125.3	−133.8	−6.7	−6.3	−16.6	−21.8
4	−158.3	−155.5	−149.0	−141.1	−7.8	−6.4	−22.0	−55.7
5	−5.6	−5.6	−5.8	−6.7	−0.2	−0.2	1.0	−1.9
6	−60.8	−59.7	−63.6	−64.0	−0.1	0.0	−1.4	−2.4
7	−9.0	−8.6	−6.8	−7.4	−1.3	−1.2	−1.7	−0.8
8	−61.0	−59.5	−59.9	−58.1	−4.4	−4.1	−7.1	0.6
9	−12.5	−12.3	−13.1	−7.8	3.1	3.1	2.0	0.6
10	−25.0	−24.7	−27.0	−28.7	1.0	1.0	−4.5	−7.7
11	−64.7	−63.2	−65.5	−64.6	−15.5	−15.2	−16.6	−20.9
12	−169.7	−166.2	−171.1	−167.9	−23.8	−22.8	−18.1	−46.1

state predicts the LRT values well, we can use the predicted charge movements of this transition to explain relative differences in g_{xy}.

Classical Interpretations. The $\boldsymbol{\mu}-\boldsymbol{\Theta}$ interaction has been shown to play a significant role in the overall OR of an oriented system.[19,20,35g] We split g_{xy} into components associated with the magnetic dipole g^{m}_{xy} and the electric quadrupole g^{Θ}_{xy} (Table 2). Exclusion of the g^{Θ}_{xy} contribution from the HOMO → LUMO g_{xy} brings greater correspondence with LRT by |3%| on average. Thus, the quadrupole contribution neither aids nor hinders the interpretation for this group of compounds. It is conveniently ignored.

Compound **2** is an exception. The aim of including **2** was to consider the complication of competing σ electrons by substituting four hydrogen atoms in **1** by four methyl groups in **2**. At first blush, g_{xy} does not change much, indicating the unimportance of the σ system, but this would be an infelicitous interpretation. For **2** only, g^{Θ}_{xy} is larger in the $\pi \rightarrow \pi^*$ and HOMO → LUMO g_{xy} tabulations (Table 2).

To use classical physics to describe the qualitative differences in OR, we must first determine how the geometry of the molecule affects transition electric dipole moments ($\boldsymbol{\mu} = qd$) and transition magnetic dipole moments ($\mathbf{m} = IA$),[40] where q is charge, d is distance, I is current, and A is area. Generally speaking, the larger the conjugated ribbon, the larger the charge separation and circulation; therefore, the larger the OR. For instance, **6** > **5**, **8** > **7**, **10** > **5**, and **12** > **6**. Here follows more particular comparisons drawn from Table 1: (1) Charge separation of **4** is larger than **3**; however, the overall circulation is relatively unchanged, as judged from the equivalent magnetic moments. The increase in charge separation results in a higher g_{xy} for **4**. (2) The OR of **5** is less than half of **1**, despite the comparable diene structures. This is presumably because of the diminished $\boldsymbol{\mu}$ (Table 3) that is a consequence of ring closure, bringing C_1 and C_4 closer in **5**. (3) The responses of **5** and **7** are identical, despite the extension of the π-system. This illustrates the predominance of the HOMO−LUMO transition; **7** has zero HOMO coefficients on the carbon atoms in the exocyclic double bond (Figure 2). This leads to comparable charge distributions for both **7** and **5**. The same can be said for **6** compared with **8**. (4) The π topology of **9** and **10** is comparable, as are topologies of **11** and **12**, but in each pair, the compound with the largest separation between terminal carbons has a correspondingly larger OR.

Table 3. Absolute Values of Computed Transition Moments in a.u[a]

	633 nm, aug-cc-pVDZ		
	$\boldsymbol{\mu}_y$[b]	$\mathbf{m}_z$[c]	$\boldsymbol{\Theta}_{xy}$[d]
1	1.5	0.5	4.2
2	1.4	0.2	7.6
3	2.0	1.2	4.9
4	2.7	1.2	10.9
5	0.8	0.5	2.2
6	0.8	1.1	1.2
7	0.3	0.5	1.2
8	0.4	1.0	0.3
9	0.7	0.5	0.7
10	2.2	0.6	2.7
11	1.2	0.7	6.3
12	1.9	0.8	6.5

[a]Hückel HOMO → LUMO. [b]Electric dipole moment is in the $-y$ direction. [c]Magnetic dipole is in the $+x$ direction. [d]Only the yz component of the quadrupole moment is symmetry-allowed.

But, what of the sign? In other words, what makes for the direction of the azimuthal rotation of plane polarized light, and can we properly predict this rotation from just the HOMO → LUMO transition? Figure 3 illustrates how rotation is reckoned in fulvene **7**. For the Hückel HOMO → LUMO excitations and the transition dipole moments, all we need for a credible interpretation, μ points in the $-y$ direction and m points in the $+x$ direction. We stress that only the relative phases of the moments matter, not the absolute signs. If an incident light wave (k) enters the molecule from the $[+x,+y]$ direction in Figure 3a, the result will be observed from $[-x,-y]$ as if viewing the light source. If positive charge is driven from right to left in the $-y$ direction, counterclockwise around the path of conjugation, the magnetic dipole will point in the $+x$ direction according to the coordinate system in Scheme 1. The moments so generated will make antiparallel projections onto the wave vector, k_{xy}. The E_k and H_k fields of the light must be able to excite μ and m some of the time. Take E_k in the $+z$ direction. H_k points in the $[-x,+y]$ direction (Figure 3a). According to Faraday's Law of Induction, a magnetic moment will be generated in the opposite direction of the field producing it; H_k has a component in the $-x$ direction, generating m in the $+x$ direction. Since H_k must also have a projection in the $+y$ direction, it generates an electric dipole proportional to $-\partial H/\partial t$[41] in the $-y$ direction.

DOI: 10.1021/jacs.5b01763
J. Am. Chem. Soc. 2015, 137, 5177−5183

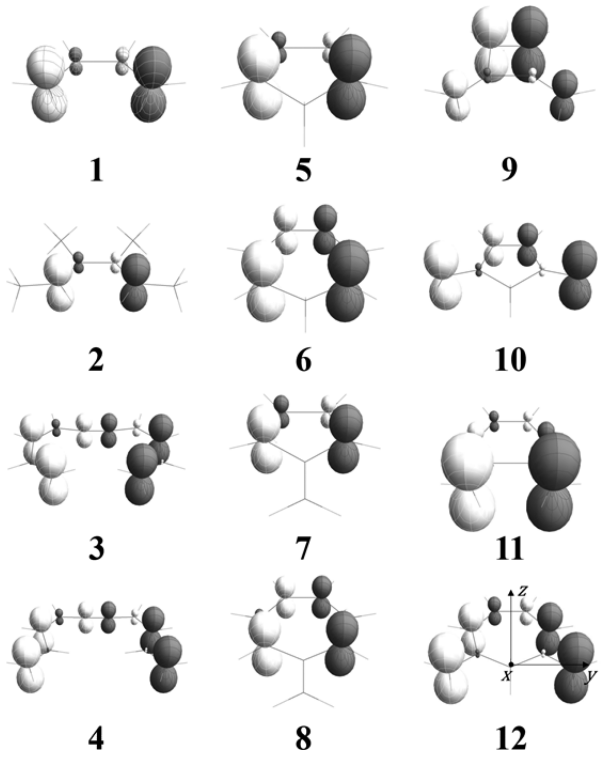

Figure 2. Overlap densities for HOMO → LUMO states. Gray (white) indicates charge enhancement (depletion).

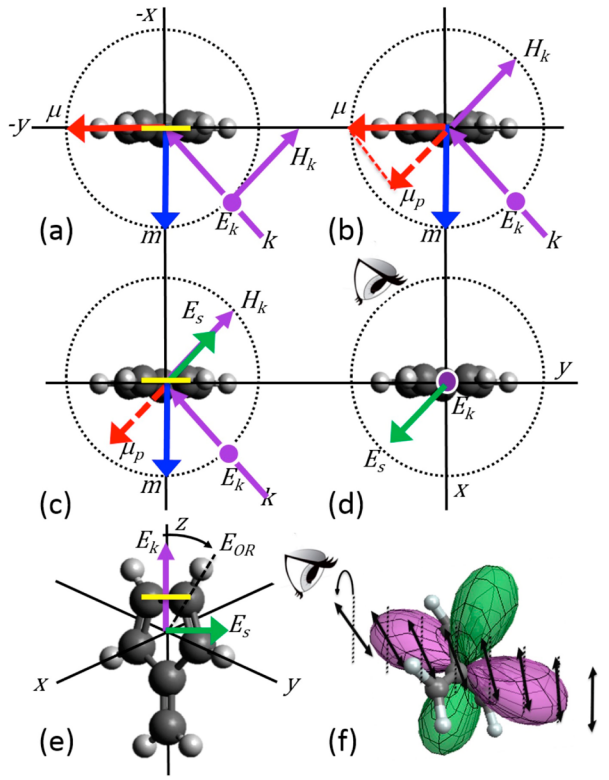

Figure 3. Generation of moments from an incident light beam (k_{xy}) showing how scattered light from **7** leads to dextrorotation in a C_{2v} molecule. (a) Moments $\boldsymbol{\mu}$ and **m** generated by *k*. A yellow line segment marks the cyclopentyl end of the molecule so that it can be oriented quickly with respect to part e, in which the molecule is now in 3/4 profile instead of edge on. (b) Projection of $\boldsymbol{\mu}$ (μ_p) antiparallel to H_k. (c) Generation of scattered electric field (E_s) antiparallel to μ_p; (d) E_s after retardation due to time derivatives and refringent scattering. (e) View of fields from $[-x,-y]$. (f) Tensor representation surface and rotation of linearly polarized light for **7**. Purple (green) corresponds to negative (positive) gyration and therefore dextrorotation (levorotation). Electric field enters from the lower right and undergoes a dextrorotation by convention according to the observing eye.

The OR sign depends on the direction of the scattered electric field (E_s) that is produced by μ. There is a projection of the electric dipole moment (μ_p) that is antiparallel to H_k (Figure 3b). That projection will produce E_s that has been retarded by a factor of $\pi/2$ because the moments are time derivatives of the incident plane waves. However, E_s is further retarded by another factor of $\pi/2$ as a consequence of refringent scattering,[37,41] the process whereby scattered wavelets from a plane recombine to form a secondary wave, and therefore, E_s becomes parallel to μ_p.[41] This leaves the original electric field E_k in the $+z$ direction and the scattered field E_s in the $[+x,-y]$ direction (Figure 3d). The resultant of E_k and E_s is the field E_{OR} that will be observed from $[+x,-y]$. When we rotate the molecule to better see these vectors from that perspective (Figure 3e), using the yellow bar as a marker of the cyclopentyl edge of **7**, we see that the plane of polarization has rotated clockwise, a dextrorotation by convention. This corresponds to a negative g_{xy} tensor component (Figure 3f) due to the change in sign when converting gyration to OR (eq 19). Only scattered radiation with a component orthogonal to the driving field and in-phase or out of phase ($n\pi$, where n = 0, 1, 2, 3, ...) will lead to a rotation. Intermediate phase relationships (e.g., $n\pi/2$ where n = 1, 3, 5, ...) will lead to ellipticity. On the other hand, for k_{-xy}, H_k can produce only parallel projections of the moments onto the light vector, and therefore, we observe levorotation from $[+x,-y]$; the sign of the response must change each time the observer crosses over a molecular mirror plane, as in solution where the dot product $\boldsymbol{\mu}\cdot\mathbf{m}$ is consequential in determining sign.

The picture above, however, is not complete because it gives pride of place to E_z. In reality, E can be oriented in any plane perpendicular to k and the same OR will be measured; the azimuthal orientation of the light wave does not matter. This experimental fact has long been reckoned with Fresnel's construction that takes linearly polarized light as the superposition of two counter-propagating circular eigenstates. However, one can construct a reciprocal picture for E_k in the xy plane, in which a scattered magnetic field component is likewise generated.

CONCLUSION

The optical activity of oriented, achiral, C_{2v}-symmetric conjugated dienes, trienes, tetraenes, and pentaenes can be estimated using nothing more than the characteristics of the HOMO and LUMO derived from simple Hückel theory. In this way, we have subverted for this class of compounds the vexing SOS problem that has plagued the interpretation of long-wavelength OR and connected the circular birefringence to the real electronic structure of an important class of organic compounds. This leads to some recommendations for teachers of a first course in organic chemistry. (1) Continue to introduce optical activity as a method for detecting chiral molecules in solution and establishing enantiopurity, but return to the subject when discussing the electronic structure of conjugated hydrocarbons to explain how OR works for a real molecule such as cyclopentadiene. All that is necessary is to knowledge the qualitative form of the HOMO and the LUMO. For instance, Figure 1 shows how the overlap density arises from the HOMO

DOI: 10.1021/jacs.5b01763
J. Am. Chem. Soc. 2015, 137, 5177−5183

and LUMO, the relationship of the moments that are generated, and how the projections of these moments onto a light vector can predict the sense of the rotation of linearly polarized light. (2) Do not cite enantiomorphism as a necessary condition for optical activity.[18] It is not, as is well-known in the community of crystal physicists. Gyration tensor elements for nonenantiomorphous Laue groups are explicitly given in standard texts.[42] In fact, by treating wave functions of planar molecules, the mechanisms of optical activity become transparent, in contrast to the intrinsically twisted wave functions of chiral molecules. Once we break the infelicitous linkage of chirality and optical activity, we can begin to more fully articulate chiroptical mechanisms.

■ ASSOCIATED CONTENT

Supporting Information

Complete Gaussian reference, Cartesian coordinates for all structures, chiroptical outputs including dipole moments, full linear response and sum-overstate gyration tensors, rotatory strength tensors, SOS graphs, Gaussian orbitals, Hückel orbitals, and overlap densities. This material is available free of charge via the Internet at http://pubs.acs.org.

■ AUTHOR INFORMATION

Corresponding Author

*bart.kahr@nyu.edu

Notes

The authors declare no competing financial interest.

■ ACKNOWLEDGMENTS

B.K. thanks the NSF (CHE-0845526, DMR-1105000), and V.L.M. acknowledges a Margret Kramer Fellowship for support of this research. We thank James Cheeseman and Laurence Barron for their helpful correspondence. This research was enabled by the High Performance Computing recourses at New York University and New York University Abu Dhabi.

■ REFERENCES

(1) Biot, J. B. *Bull. Soc. Philomath.* **1815**, 190.
(2) Arteaga, O.; Freudenthal, J. H.; Kahr, B. *J. Appl. Crystallogr.* **2012**, *45*, 279.
(3) Arteaga, O.; Freudenthal, J.; Wang, B.; Kahr, B. *Appl. Opt.* **2012**, *51*, 6805.
(4) Kuball, H.-G. *Chirality* **2000**, *12*, 278.
(5) Kobayashi, J.; Asahi, T. *Proc. SPIE* **2000**, *4097*, 25.
(6) Harada, T.; Hayakawa, H.; Kuroda, R. *Rev. Sci. Instrum.* **2008**, *79*, 073103.
(7) Kaminsky, W. *Rep. Prog. Phys.* **2000**, *63*, 1575.
(8) Polavarapu, P. L. *Chirality* **2002**, *14*, 768.
(9) Stephens, P. J.; McCann, D. M.; Cheeseman, J. R.; Frisch, M. J. *Chirality* **2005**, *17*, S52.
(10) Srebro, M.; Govind, N.; de Jong, W.; Autschbach, J. *J. Phys. Chem. A* **2011**, *115*, 10930.
(11) Kondru, R. K.; Wipf, P.; Beratan, D. N. *Science* **1998**, *282*, 2247.
(12) Kundrat, M. D.; Autschbach, J. *J. Chem. Theory Comput.* **2009**, *5*, 1051.
(13) Nitsch-Velasquez, L.; Autschbach, J. *Chirality* **2010**, *22*, E81.
(14) Claborn, K. Ph.D. Dissertation, University of Washington, Seattle, WA, 2006.
(15) Gibbs, J. W. *Am. J. Sci.* **1882**, *23*, 460.
(16) Voigt, W. *Ann. Phys.* **1905**, *18*, 645.
(17) Futama, H.; Pepinsky, R. *J. Phys. Soc. Jpn.* **1962**, *77*, 725.
(18) O'Loane, K. *Chem. Rev.* **1980**, *80*, 41.
(19) Hansen, A. E.; Bak, K. L. *J. Phys. Chem. A* **2000**, *104*, 11362.
(20) Kongsted, J.; Pedersen, T. B.; Osted, A.; Hansen, A. E.; Mikkelsen, K. V.; Christiansen, O. *J. Phys. Chem. A* **2004**, *108*, 3632.
(21) Isborn, C.; Claborn, K.; Kahr, B. *J. Phys. Chem. A* **2007**, *111*, 7800.
(22) Murphy, V. L.; Kahr, B. *J. Am. Chem. Soc.* **2011**, *133*, 12918.
(23) Claborn, K.; Cedres, J. H.; Isborn, C.; Zozulya, A.; Weckert, E.; Kaminsky, W.; Kahr, B. *J. Am. Chem. Soc.* **2006**, *128*, 14746.
(24) Claborn, K.; Isborn, C.; Kaminsky, W.; Kahr, B. *Angew. Chem., Int. Ed.* **2008**, *47*, 5706.
(25) Williams, R. *Phys. Rev. Lett.* **1968**, *21*, 342.
(26) Williams, R. *J. Chem. Phys.* **1969**, *50*, 1324.
(27) Hough, L. E.; Jung, H. T.; Krüerke, D.; Heberling, M. S.; Nakata, M.; Jones, C. D.; Chen, D.; Link, D. R.; Zasadzinski, J.; Heppke, G.; Rabe, J. P.; Stocker, W.; Körblova, E.; Walba, D. M.; Glaser, M. A.; Clark, N. A. *Science* **2009**, *325*, 456.
(28) Verbiest, T.; Kauranen, M.; Van Rompaey, Y.; Persoons, A. *Phys. Rev. Lett.* **1996**, *77*, 1456.
(29) Plum, E.; Liu, X. X.; Fedotov, V. A.; Chen, Y.; Tsai, D. P.; Zheludev, N. I. *Phys. Rev. Lett.* **2009**, *102*, 113902.
(30) Wiberg, K. B.; Wang, Y.-g.; Wilson, S. M.; Vaccaro, P. H.; Cheeseman, J. R. *J. Phys. Chem. A* **2006**, *100*, 13995.
(31) Kunrat, M. D.; Autschbach, J. *J. Am. Chem. Soc.* **2008**, *130*, 4404.
(32) Autschbach, J. *ChemPhysChem* **2011**, *12*, 3224.
(33) Moore, B., II; Srebro, M.; Autschbach, J. *J. Chem. Theory Comput.* **2012**, *8*, 4336.
(34) Lahiri, P.; Wiberg, K. B.; Vaccaro, P. H.; Caricato, M.; Crawford, D. T. *Angew. Chem., Int. Ed.* **2014**, *53*, 1386.
(35) (a) Polavarapu, P. L. *Mol. Phys.* **1997**, *91*, 551. (b) Kondru, R. K.; Wipf, P.; Beratan, D. N. *Science* **1998**, *282*, 2447. (c) Cheeseman, J. R.; Frisch, M. J.; Devlin, F. J.; Stephens, P. J. *J. Phys. Chem. A* **2000**, *104*, 1039. (d) Stephens, P. J.; Devlin, F. J.; Cheeseman, J. R.; Frisch, M. J. *J. Phys. Chem. A* **2001**, *105*, 5356. (e) Ruud, K.; Helgaker, T. *Chem. Phys. Lett.* **2002**, *352*, 533. (f) Tam, M. C.; Russ, N. J.; Crawford, T. D. *J. Chem. Phys.* **2004**, *121*, 3550. (g) Kongsted, J.; Pedersen, T. B.; Strange, M.; Osted, A.; Hansen, A. E.; Mikkelsen, K. V.; Pawlowsi, F.; Jorgensen, P.; Hattig, C. *Chem. Phys. Lett.* **2005**, *401*, 385. (h) Crawford, T. D.; Stephens, P. J. *J. Phys. Chem. A* **2008**, *112*, 1339. (i) Autschbach, J. *Chirality* **2009**, *21*, E116. (j) Barron, L. D.; Buckingham, A. D. *Chem. Phys. Lett.* **2010**, *492*, 199. (k) Polavarapu, P. L. *Chirality* **2012**, *24*, 909. (l) McAlexander, H. R.; Mach, T. J.; Crawford, T. D. *Phys. Chem. Chem. Phys.* **2012**, *14*, 7830. (m) Wiberg, K. B.; Caricato, M.; Wang, Y. G.; Vaccaro, P. H. *Chirality* **2013**, *25*, 606.
(36) Snatzke, G. *Angew. Chem., Int. Ed.* **1979**, *18*, 363.
(37) Barron, L. D. *Molecular Light Scattering and Optical Activity*; Cambridge University Press: New York, 2004.
(38) Pedersen, T. B.; Hansen, A. E. *Chem. Phys. Lett.* **1995**, *246*, 1.
(39) Buckingham, A. D.; Dunn, M. B. *J. Chem. Soc. A* **1971**, 1988.
(40) Feynman, R. P. *The Feynman Lectures on Physics*; Addison-Wesley: Reading, MA, 1963; Vol. *II*, pp 14−18.
(41) Kauzmann, W. *Quantum Chemistry: An Introduction*; Academic Press, New York, 1957.
(42) Nye, J. F. *Physical Properties of Crystals: Their Representation by Tensors and Matrices*; Oxford University Press: Oxford, 1979.

DOI: 10.1021/jacs.5b01763
J. Am. Chem. Soc. 2015, 137, 5177−5183